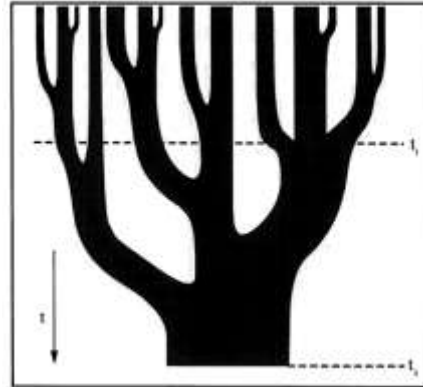
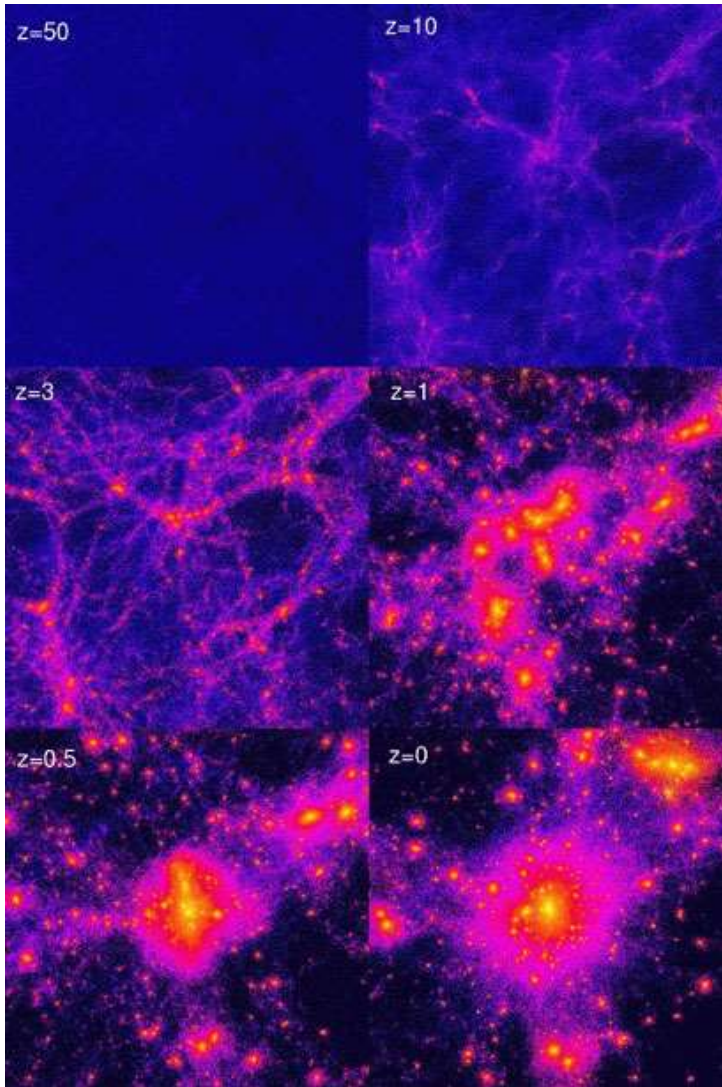


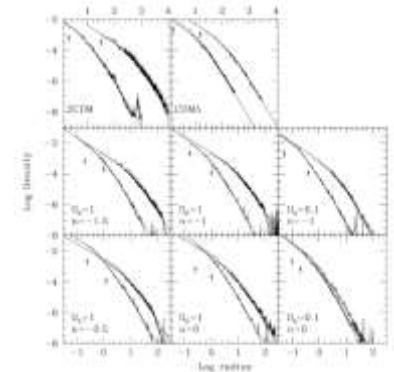
銀河スケールのダークマターハローの スケーリング則について

森 正夫

Structure formation in the CDM universe



Lacey & Cole 1993

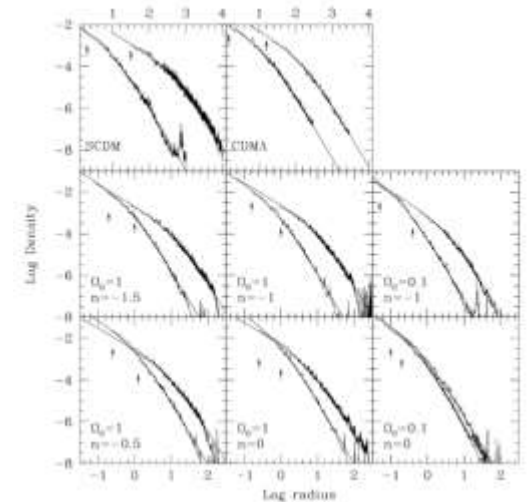
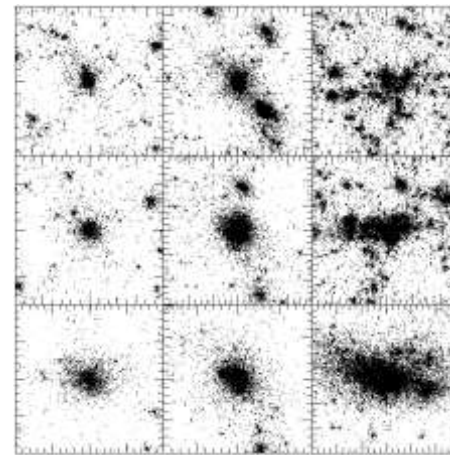
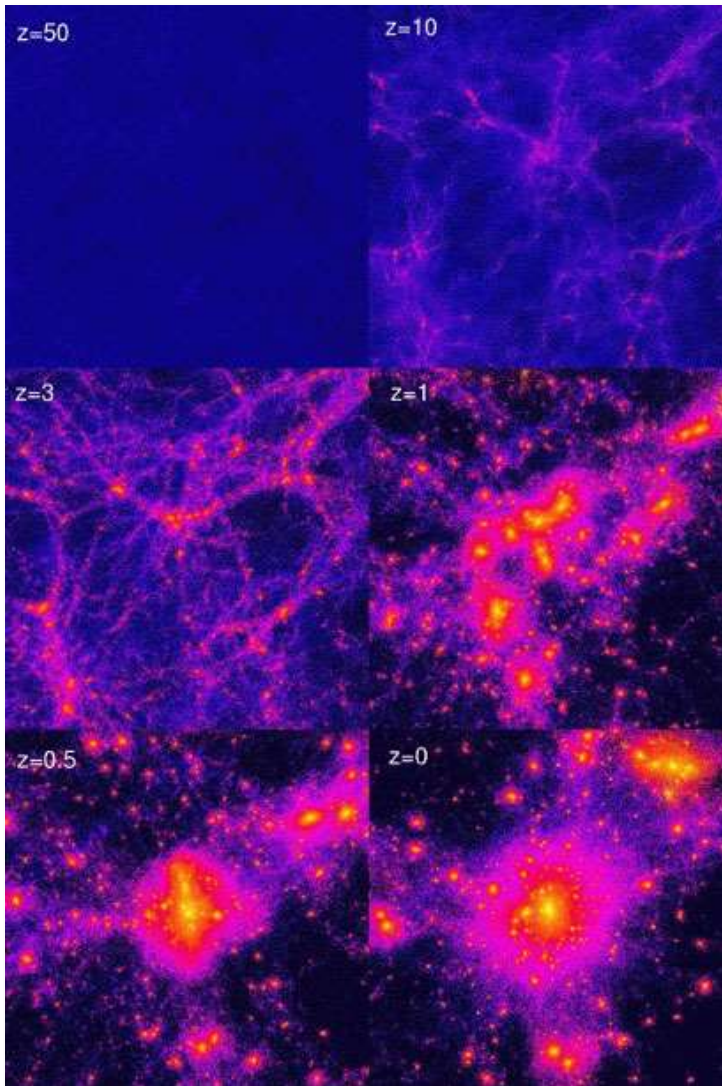


Navarro, Frenk & White, 1997

標準的な構造形成理論である cold dark matter(CDM)モデルは、宇宙の大規模構造の統計的な性質を再現することに成功したが、銀河スケール以下の構造でいくつかの問題が存在する。

- ミッシングサテライト問題
- カスプコア問題
- Too-big-to-fail問題
- ...

Structure formation in the CDM universe



Navarro, Frenk & White, ApJ, 490, 493 (1997)

NFW profile
$$\frac{\rho(r)}{\rho_{\text{crit}}} = \frac{\delta_c}{(r/r_s)(1 + r/r_s)^2}$$

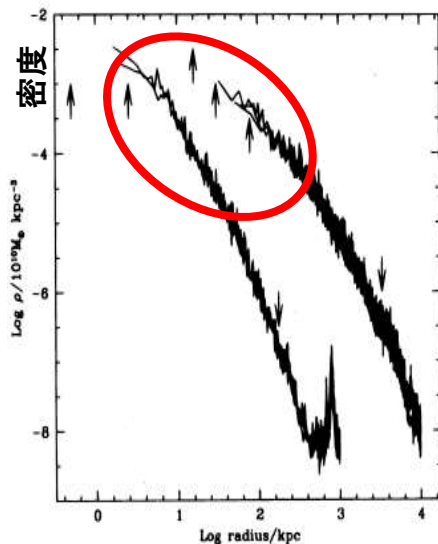
中心付近の密度は、 $\rho \propto r^{-1}$

Cusp-core問題とToo-big-to-fail問題

Cusp-core問題

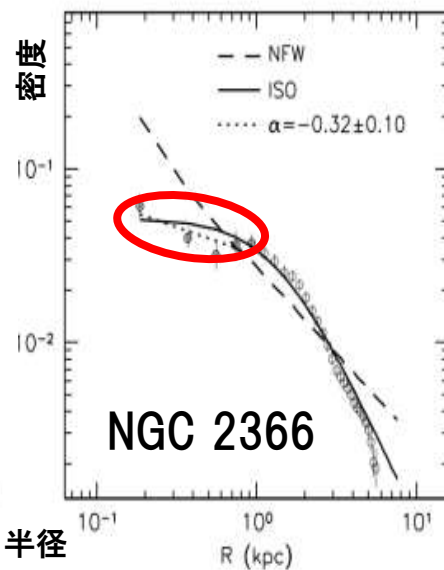
dark matter halo の中心密度分布の矛盾

理論: cusp構造
(中心密度分布が発散)



Navarro et al. (1996)

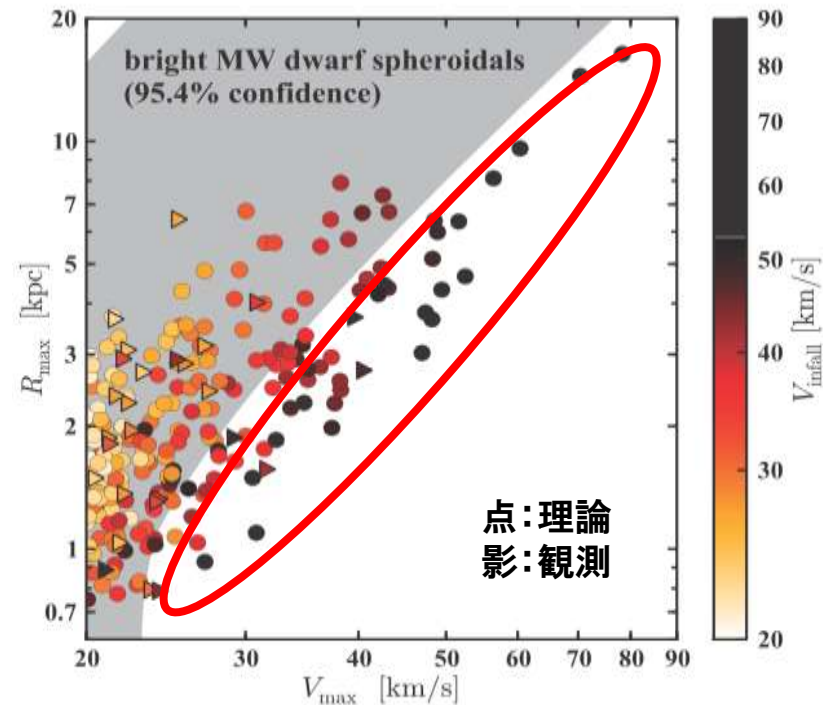
観測: core構造
(中心密度分布が平坦)



Oh et al. (2011)

Too-big-to-fail問題

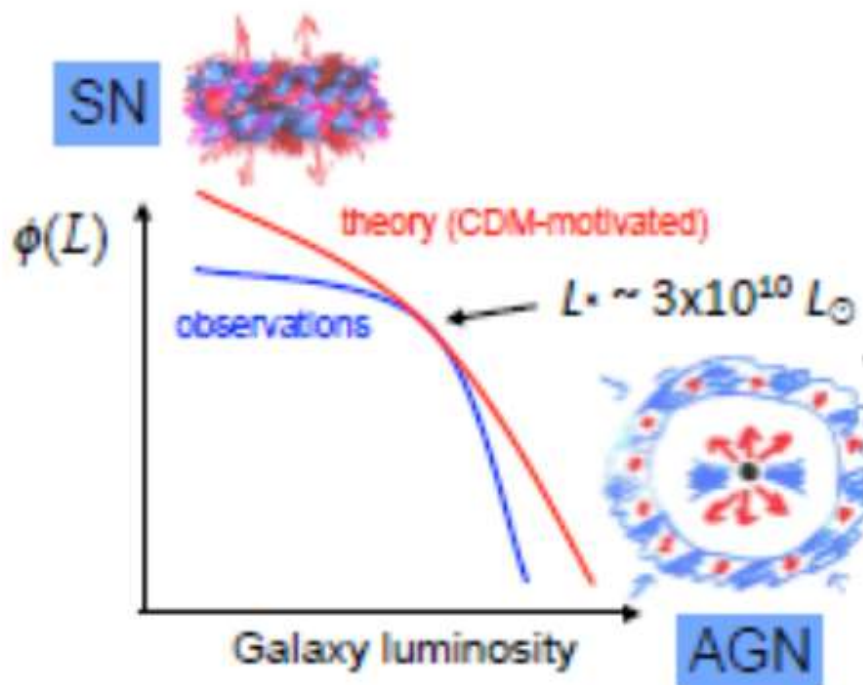
理論で予言される中心密度が高いDMHが、観測されていない



Boylan-Kolchin et al.(2011)

フィードバック問題 II

5



Silk & Mamon 2012

- Stellar feedback
超新星等によりISMが加熱され、大規模な質量放出が発生し、星形成を抑制
- Photoheating from UV background
- AGN feedback
AGNがエネルギーを放出し星形成を抑制

銀河からのアウトフロー

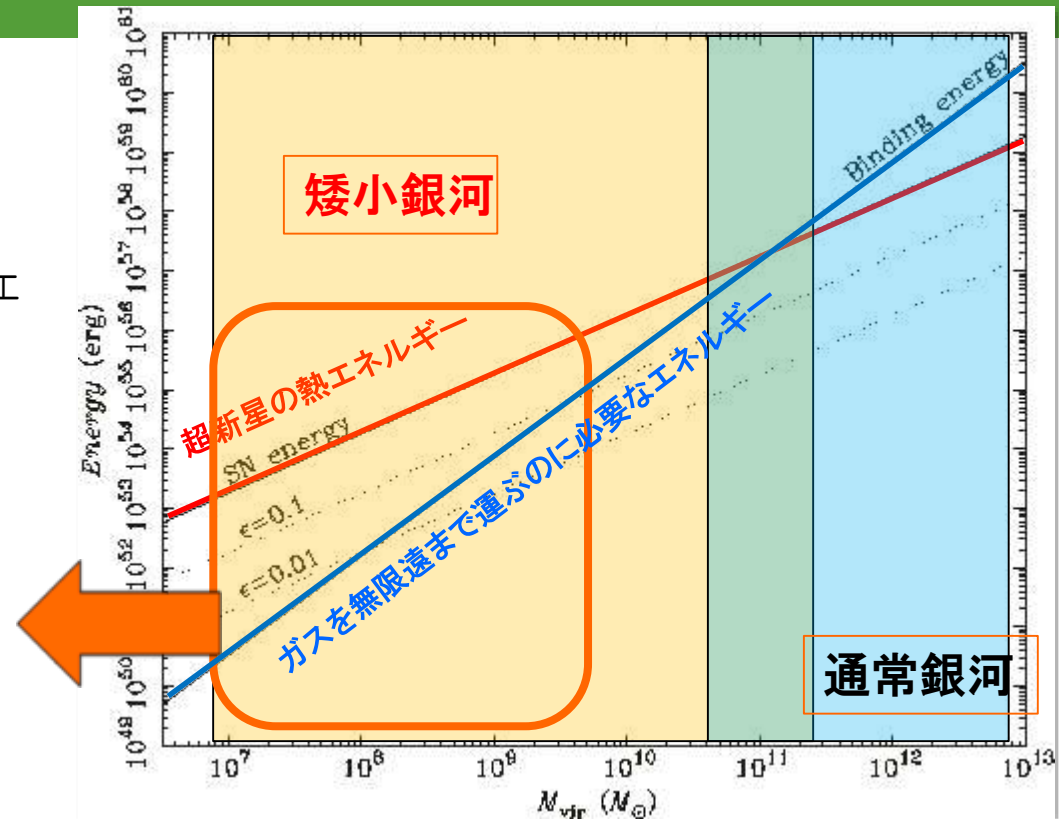
Mori et al. 1997, 1999, 2002

- 銀河全体の重力ポテンシャルエネルギー: $E_g = E(M)$
※NFW プロファイルを仮定
- 銀河内の全超新星によって発生する熱エネルギー:

$$E_t = E(M)$$

※全質量の1%が短時間で星になったとした場合

- 超新星の熱エネルギーが卓越
- 圧力勾配によりガスの流出
- 銀河風の発生
- 大質量のガスの放出
- 星形成の抑止
- 銀河形成が終わる



銀河の総質量 M

➡ Negative Effect: 輻射輸送による熱エネルギーの散逸?

Positive Effect: 超新星によって放出されたガスから星形成?

➡ **現実的な数値シミュレーション**

銀河形成・進化シミュレーション

7

- N-body 重力多体問題(ダークマター、星)
- 流体力学、放射冷却 (Katz & Gunn 1991, Evrard 1993, 他)
- 星形成、超新星爆発 (Katz 1992, Navarro & White 1993, 他)
- 化学進化(重元素放出、ガスとのmixing)
Steinmetz & Müller (1994), Raiteri et al (1996) 他
- 光学進化(種族合成モデルとの結合、ダスト)
Mori et al (1997), Contardo et al (1998), Bekki & Shioya (1998) 他
- 輻射輸送 (Abel et al. 1999, Susa & Umemura 2004, 他)
- 非平衡過程、ダスト放射 (Yajima+ 2012, 他)
- ダスト進化 (ダストの形成、破壊)
Bekki (2015), McKinnon, Torrey & Vogelsberger (2016),
Aoyama et al. (2017)

Dark Matter Heating and Early Core Formation in Dwarf Galaxies

Shen et al 2014, Madau & Shen 2014

They present results from a fully cosmological, very high-resolution, Λ CDM simulation of a group of seven field dwarf galaxies with present-day virial masses in the range $M_{\text{vir}} = 4.4 \times 10^8 - 3.6 \times 10^{10} M_{\text{sun}}$.

- The zoom-in simulation was performed with the parallel TreeSPH code Gasoline (Wadsley et al. 2004) in a $\Omega_M = 0.24$, $h = 0.73$, $\sigma_8 = 0.77$, and $\Omega_b = 0.042$ cosmology.
- The high resolution region, about 2 Mpc on a side at $z = 0$, was embedded in a low-resolution dark matter-only periodic box of 25 Mpc on a side.
- It contains about 6 million dark matter and an equal number of SPH particles, with particle masses of $m_{\text{DM}} = 1.6 \times 10^4 M_{\text{sun}}$ and $m_{\text{SPH}} = 3.3 \times 10^3 M_{\text{sun}}$, respectively.
- The gravitational spline softening length for collisional and collisionless particles was fixed to $\epsilon = 86$ pc (physical). In high density regions the gas smoothing length is allowed to shrink to 0.1ϵ to ensure that hydrodynamic forces are well resolved on small scales.

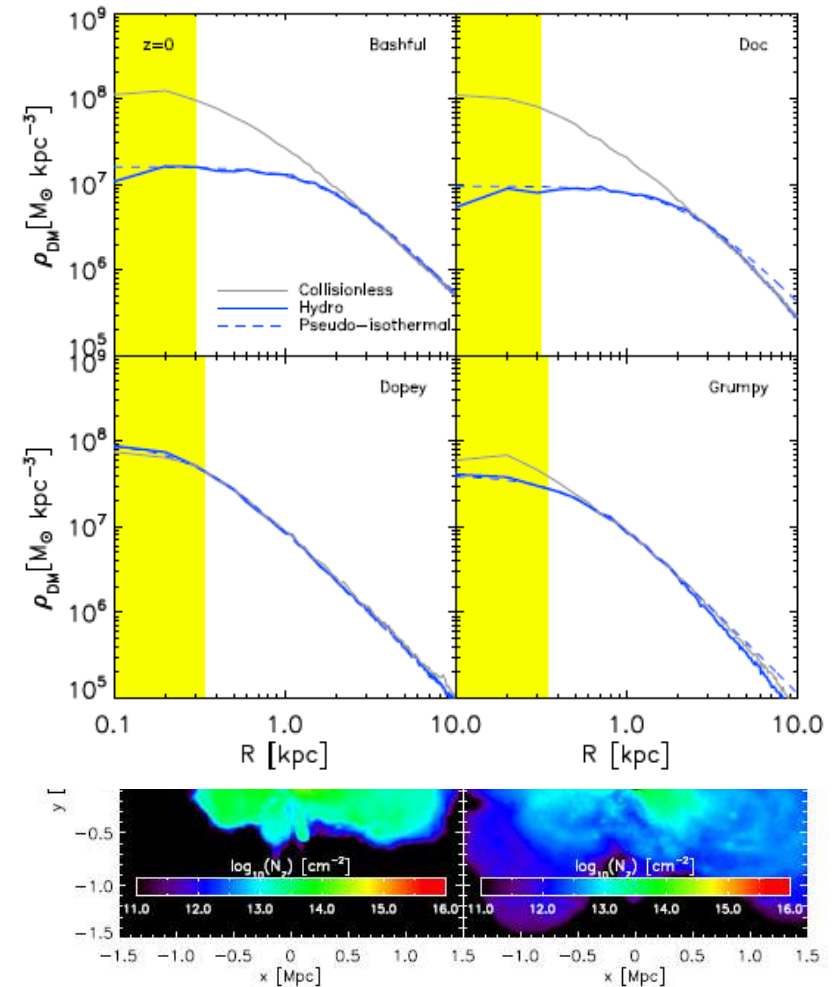
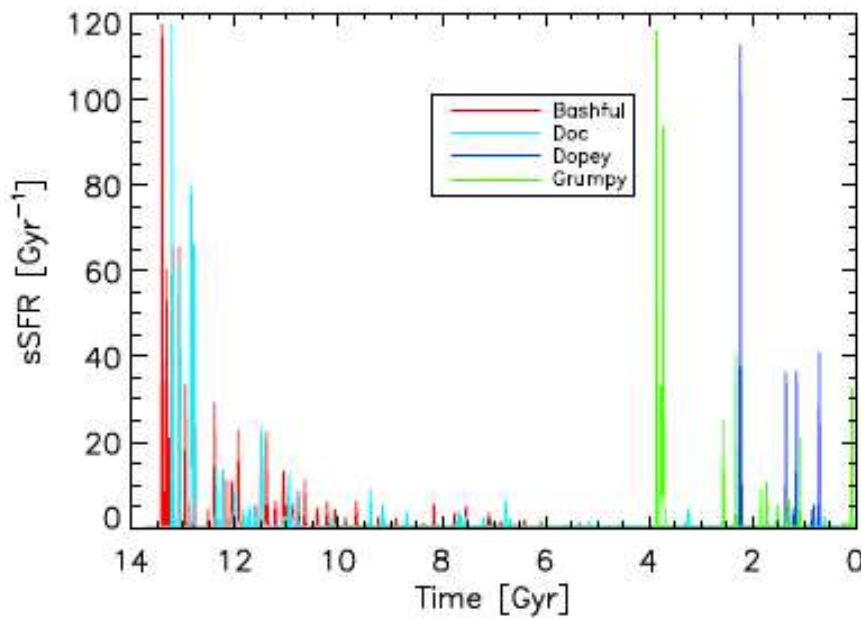
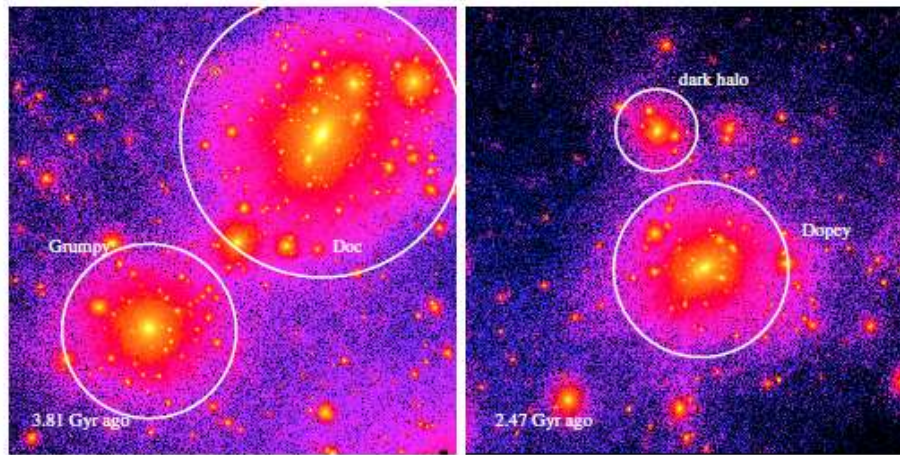
The simulation includes:

- collisionless dynamics (dark matter and stars) and gas dynamics (SPH)
- metal-dependent radiative cooling
- uniform UV background
- star-formation recipe based on a high gas density threshold (100 atm/cc)
- blastwave scheme for supernova feedback.

Dark Matter Heating and Early Core Formation in Dwarf Galaxies

Shen et al 2014, Madau & Shen 2014

9

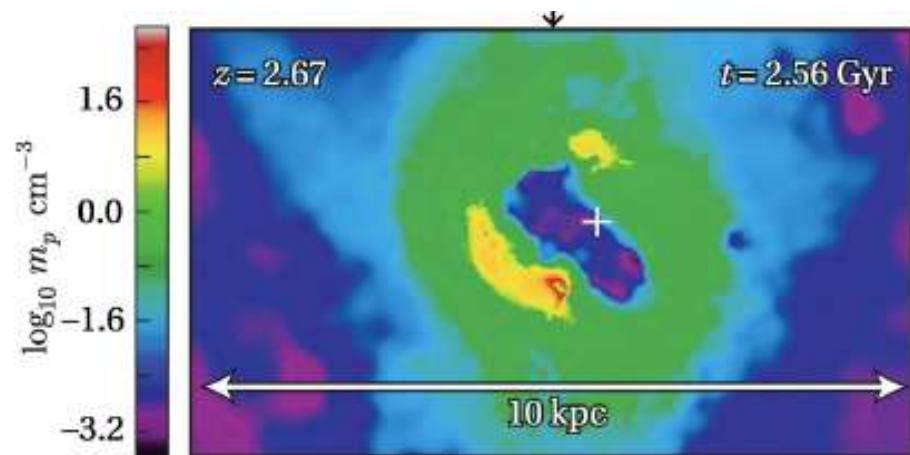


Shen et al. 2014; Madau & Shen 2014

Effect of baryonic processes in less-massive galaxies

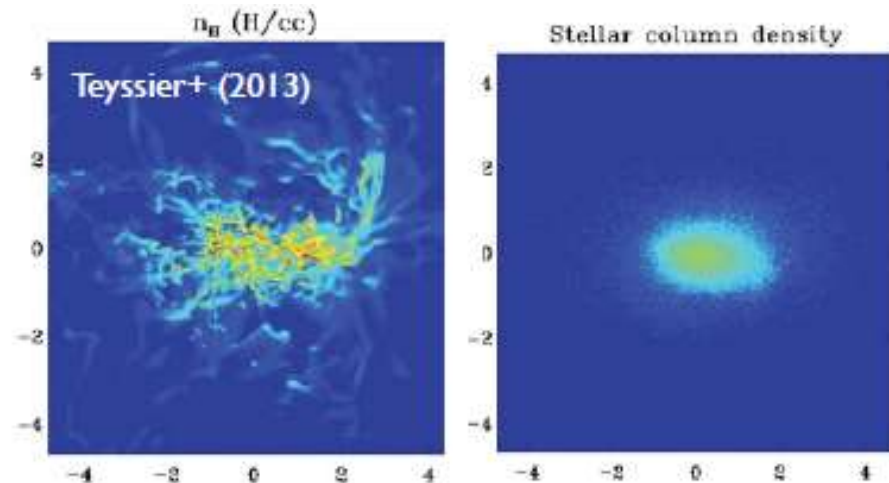
- 低質量銀河では重力ポテンシャルが小さいため、星形成に伴って発生する超新星爆発により、大規模なガスのアウトフローが発生する
- フィードバックとアウトフローによる星形成の抑制
- ダークマターハローの中心コアの生成

Pontzen & Governato (2012):
Rapid change of the central potential
transform into core



Teyssier et al. (2013):

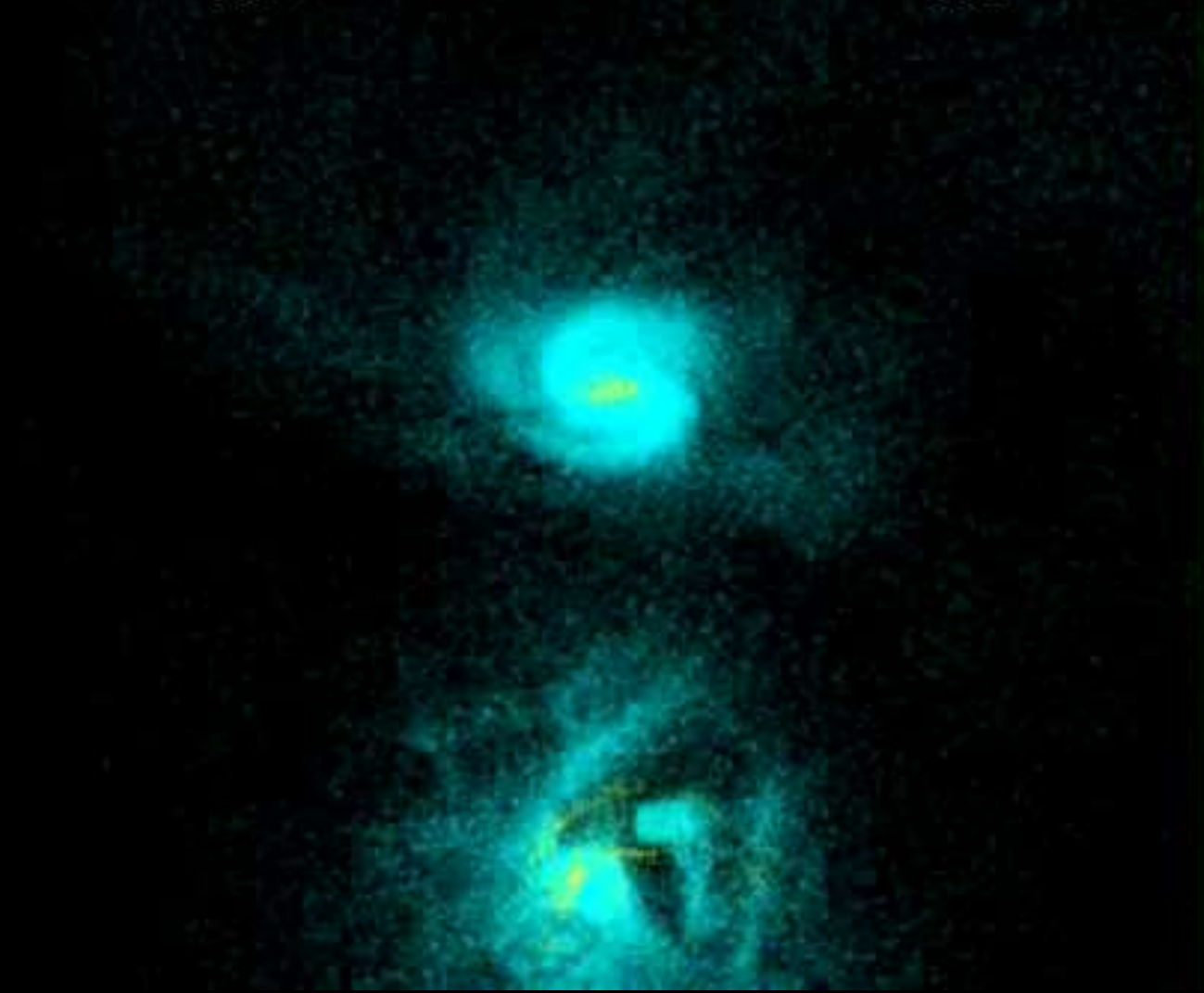
Stellar feedback create dark matter cores, and makes the stellar distribution dynamically hot.



Cosmological N-body+SPH simulation

Mashchenko et al. (2008)

0.00 0.800 $t=146$ Myr



Linear analysis: resonance model

Ogiya & Mori (2014)

- ✓ Equilibrium system (0) by external force (ex) \Rightarrow induced values (ind)
- ✓ Focus on the particle group with $\rho_0 = \text{const.}$, $v_0 = \text{const.}$

✓ External force :
$$-\frac{\partial \Phi_{\text{ex}}}{\partial r} = \sum_n A_n \cos(kr - n\Omega t)$$

(A: strength, k : wavenumber, Ω : frequency)

Linearized continuity eq. and Euler eq.

$$\begin{aligned} \frac{\partial \rho_{\text{ind}}(t, r)}{\partial t} + v_0 \frac{\partial \rho_{\text{ind}}(t, r)}{\partial r} &= -\rho_0 \frac{\partial v_{\text{ind}}(t, r)}{\partial r} & \frac{\partial v_{\text{ind}}(t, r)}{\partial t} + v_0 \frac{\partial v_{\text{ind}}(t, r)}{\partial r} &= -\frac{\partial \Phi_{\text{ex}}(t, r)}{\partial r} \\ \Rightarrow \rho_{\text{ind}}(t, r) &= -\sum_n \frac{A_n \rho_0 k}{(n\Omega - kv_0)^2} & v_{\text{ind}}(t, r) &= -\sum_n \frac{A_n}{n\Omega - kv_0} \{ \sin(kr - \Omega t) - \sin(kr - kv_0 t) \} \\ & & & \times \{ \sin(kr - n\Omega t) - \sin(kr - kv_0 t) + (n\Omega - kv_0)t \cos(kr - kv_0 t) \} \end{aligned}$$

Resonance condition:

$$n\Omega \sim kv_0$$

Resonance condition for CDM halo

- Resonance between particles and density waves

$$n\Omega \sim kv_0$$

- Some arithmetic calculations ($n = 1$)

Resonance occurs when the condition is satisfied

⇒ efficient energy transfer

⇒ system expands

⇒ **Cusp-Core transition**

$$T \approx t_d(r) = \sqrt{\frac{3\pi}{32G\overline{\rho(r)}}}$$

- CDM mass-density:

$$\rho(r) = \frac{\rho_0 R_{DM}^3}{r^\alpha (r + R_{DM})^{3-\alpha}}$$

$$r_{core} = R_{DM} \left(\frac{T}{T_c} \right)^{2/\alpha}$$

$$T_c^2 \equiv \frac{\pi^2}{8G} \frac{R_{DM}^3 c^{3-\alpha} {}_2F_1[\alpha; -c]}{M_{vir}}$$

Gauss's hyper-geometric function

Cusp-core transition driven by periodic supernova feedbacks

(Ogiya & Mori 2011, 2014; Ogiya et al. 2014)

Periodic SN feedback Model:

深いDMHポテンシャル中での星形成



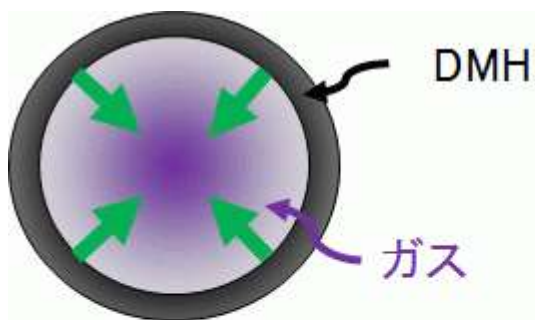
相対的に弱いSN feedback



ガスの再降着(Failed galactic-wind)



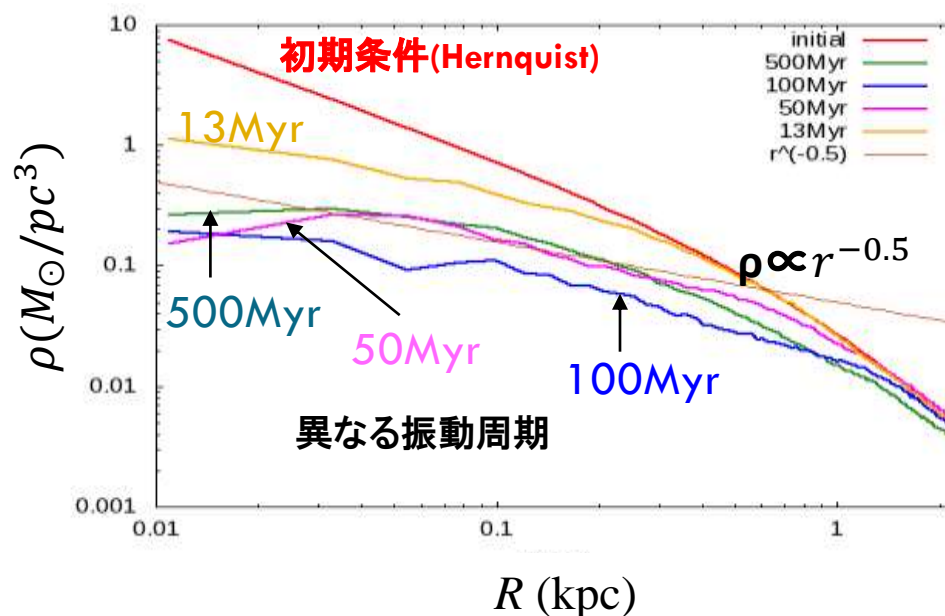
周期的な SN feedback



重力によりガス収縮

N-body simulations using “Nested Particle Mesh Method”

(Kato+ in prep.)



Periodic SN Feedbackで Cusp-Core transitionが発生することを検証。(Ogiya & Mori 2011, 2014)

- 中心付近の密度分布の冪は観測を再現
- コア半径は概ね振動周期に依存する。
(Ogiya & Mori 2014)
- 密度分布の冪は振動周期に依存しない。

Connection between “too-big-to-fail” and “cusp-core”

(Kato & Mori in prep.)

Boylan-Kolchin et al.(2011)

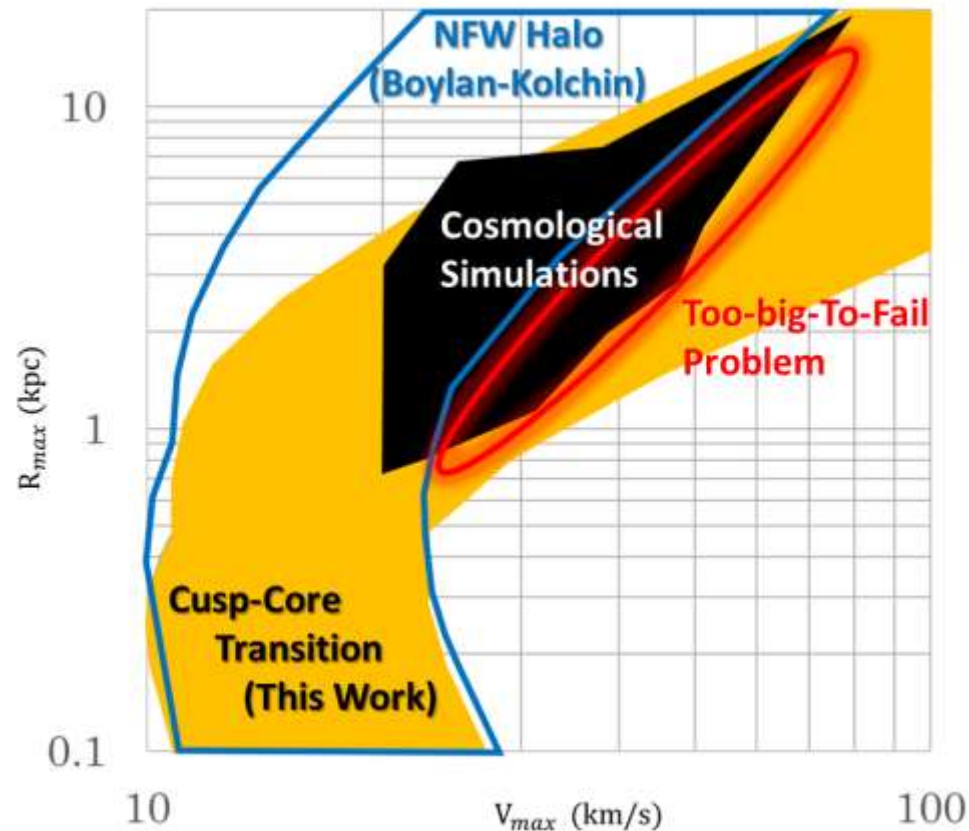
矮小銀河の回転則からDMHの質量分布を見積もる際にカスプを持つ **“NFW モデル”**を仮定。

⇒ **“Too-big-to-fail problem”**

しかし、実際には矮小銀河のDMHは“Burkertモデル”のようなコアを持つことが示唆されている。

⇒ **“Cusp-core problem”**

- 本研究では、現在の矮小銀河のDMHは銀河形成期にcusp-core遷移を経験したと仮定。
- 現在のDMHの質量分布に**“Burkertモデル”**を仮定した上で、**Cusp-core遷移する以前の“NFW halo”**の質量分布を算出(図のオレンジ内)。
- そのようなDMHはこれまでの**cosmological simulation の結果と矛盾しない**(図の赤線内)。
- Cusp-core遷移とtoo-big-to-fail問題が関係する。



超新星フィードバックが too-big-to-fail 問題と cusp-core 問題を解く鍵である

Burkert's Scaling Relation

Burkert 1995; Mori & Burkert 2000

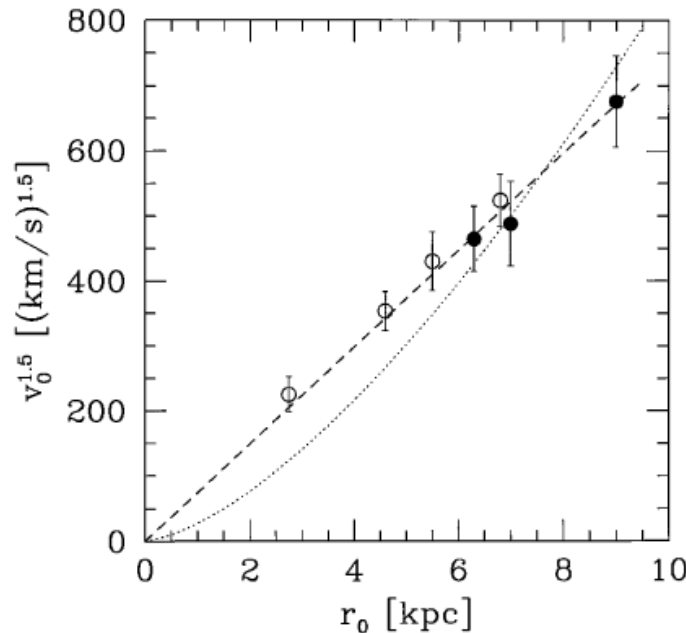


FIG. 2.—The scaling relation between the rotational velocity v_0 of the DM halos at r_0 is shown as function of the scale radius r_0 (eq. [2]). The open circles show the four best-known DDO galaxies which have been used in Fig. 1. The filled circles show three additional galaxies for which the contribution of the baryonic component to the rotation curve at r_0 had to be subtracted. The error bars show the observational uncertainty in determining v_0 as quoted in the literature. The dashed line shows a fit (eq. [3]) through the data points. An extension of the data to larger radii fits nicely the halo parameters of Sc-Irr galaxies (Kormendy & Sanders 1992). For comparison, the dotted curve shows a linear fit $v_0 \sim r_0$.

Burkert's Profile

$$\rho_d(r) = \frac{\rho_{d0} r_0^3}{(r + r_0)(r^2 + r_0^2)},$$

$$M_d(r) = \pi \rho_{d0} r_0^3 \left\{ -2 \arctan \frac{r}{r_0} + 2 \ln \left(1 + \frac{r}{r_0} \right) + \ln \left[1 + \left(\frac{r}{r_0} \right)^2 \right] \right\}.$$

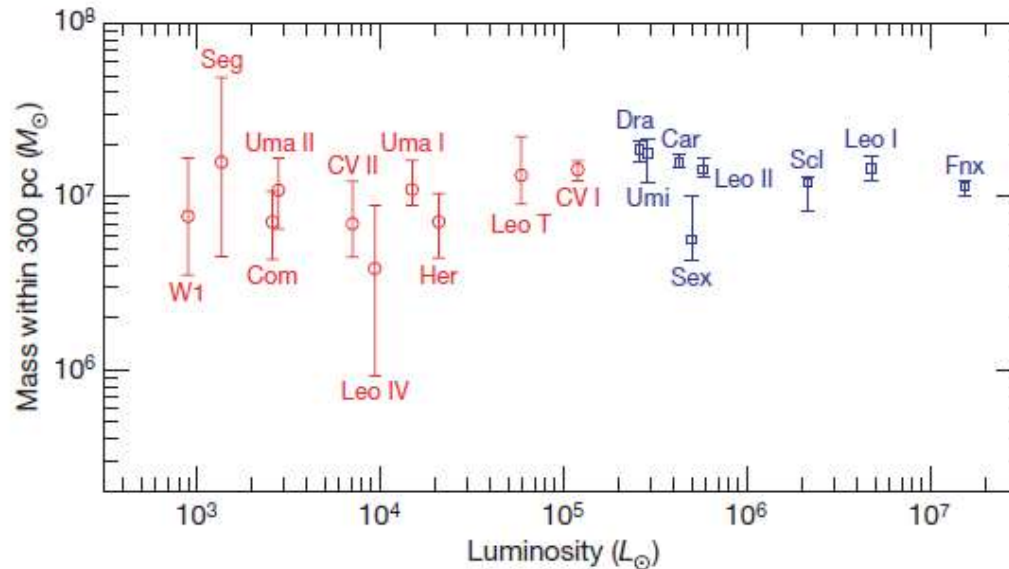
$$v_0 = 17.7 (r_0 \text{ kpc}^{-1})^{2/3} \text{ km s}^{-1},$$

$$M_0 = 7.2 \times 10^7 (r_0 \text{ kpc}^{-1})^{7/3} M_\odot,$$

$$\rho_0 = 4.5 \times 10^{-2} (r_0 \text{ kpc}^{-1})^{-2/3} M_\odot \text{ pc}^{-3}$$

A common mass scale for satellite galaxies of the Milky Way

Strigari et al., nature, 454, 1096 (2008)



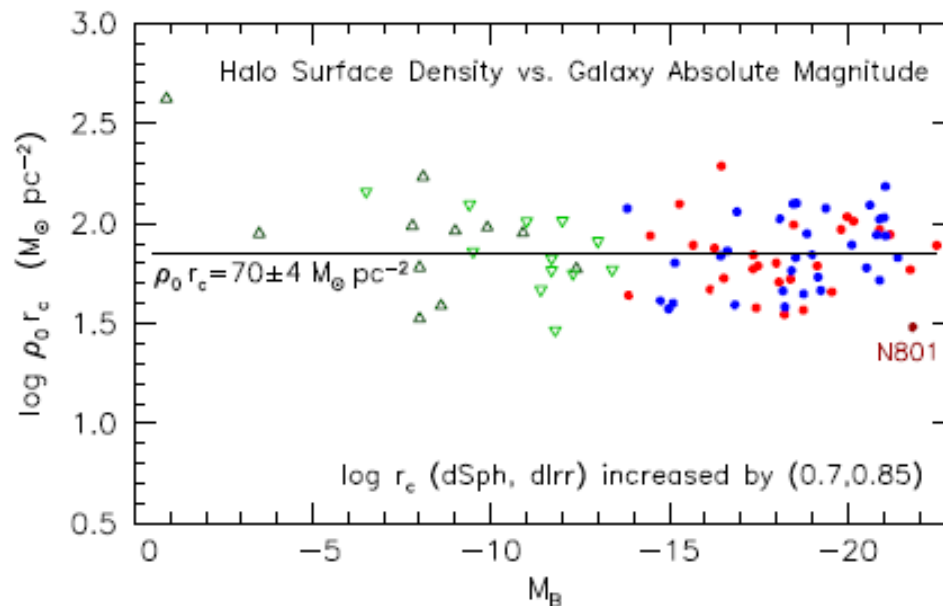
$$M(r \leq 300 \text{ pc}) = 10^7 M_\odot$$

Figure 1 | The integrated mass of the Milky Way dwarf satellites, in units of solar masses, within their inner 0.3 kpc as a function of their total luminosity, in units of solar luminosities. The circle (red) points on the left refer to the newly discovered SDSS satellites, whereas the square (blue) points refer to the classical dwarf satellites discovered pre-SDSS. The error bars reflect the points where the likelihood function falls off to 60.6% of its peak value.

Milky Way satellite galaxies are consistent with them having a common mass of about $10^7 M_\odot$ within their central 300 parsecs.

Kormendy-Freeman Relation

Kormendy & Freeman, ApJ, 817, 84 (2016)



$$\rho_0 r_c = 70 \pm 4 M_\odot \text{ pc}^{-2}$$

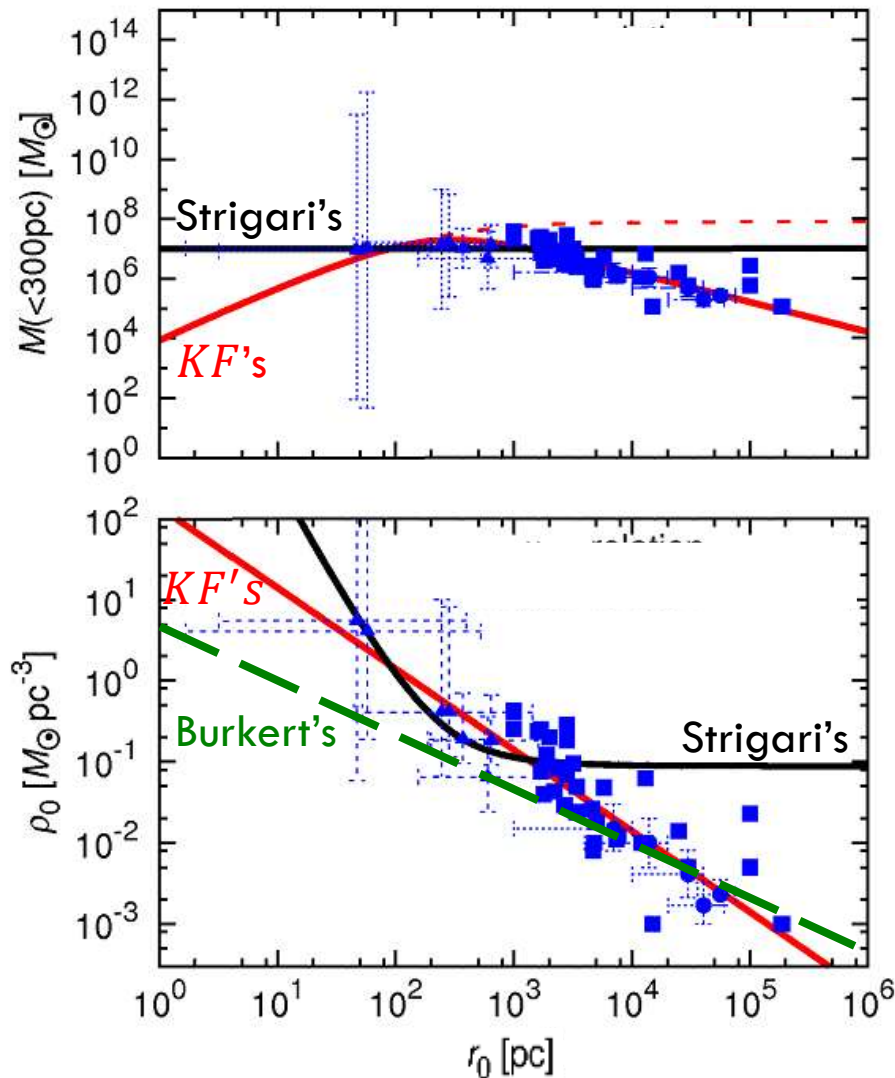
Figure 8. Product $\rho_0 r_c \propto$ surface density of DM halos as a function of observed (not shifted) absolute magnitude. Symbols are as in Figures 2–7. The straight line shows the mean surface density for the Sc–Im galaxies. The dark and light green points are for dSph and dIm galaxies, respectively. The $\log r_c$ values for their DM halos are derived from the $\log r_c$ values for their stellar or H I distributions by applying shifts as given in the key and explained above.

Central surface densities of DMHs in Sc-Im and dSph galaxies are constant from $M_B \sim -5$ to -22 .

Interconnection among these relations

Ogiya, Mori, Ishiyama & Burkert (2014)

19



Assuming Burkert profile:

$$\rho_d(r) = \frac{\rho_{d0} r_0^3}{(r + r_0)(r^2 + r_0^2)},$$

- Strigari's relation breaks in larger halos
- KF's relation keeps consistency
- The KF relation holds in the broader range
- Strigari relation is an indirect evidence of the KF relation

The connection between the cusp-to-core transformation and observational universalities of DM haloes

Ogiya, Mori, Ishiyama & Burkert 2014

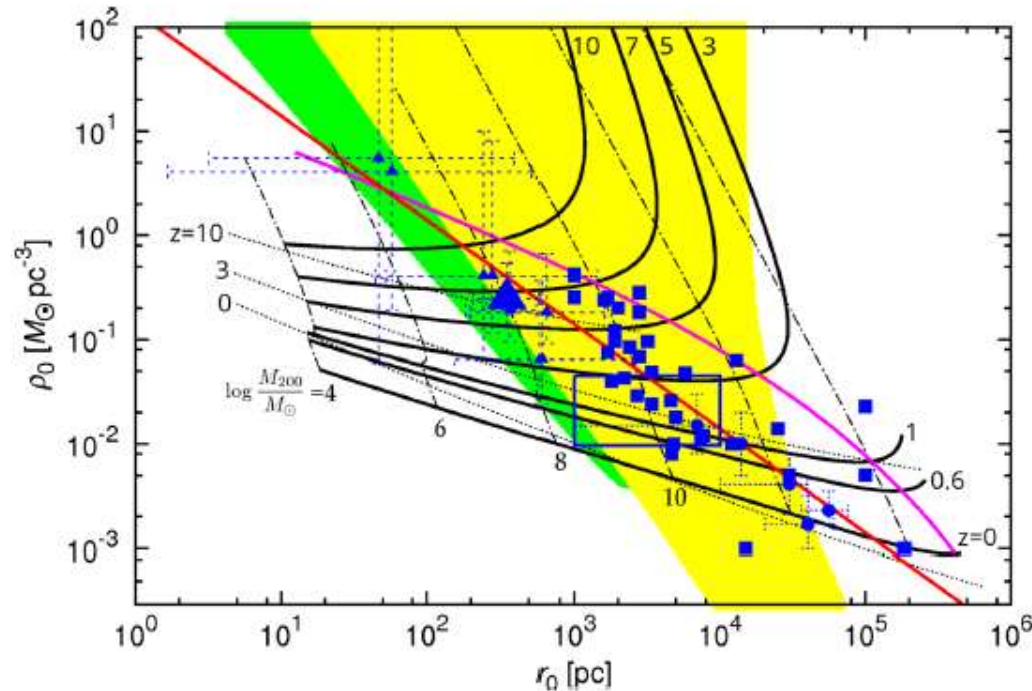


Figure 2. Diagram of r_0 versus ρ_0 . Respective points show the parameters of the Burkert profile, ρ_0 and r_0 , obtained by observations. Triangles, squares and circles represent the data from Salucci et al. (2012), Spano et al. (2008) and Donato et al. (2009), respectively. Large triangle denotes the Sculptor dSph. Red line is the scaling relation between ρ_0 and r_0 proposed by Salucci et al. (2012). The place embraced by blue box corresponds to the results of Burkert (1995). Solid and dotted black lines show the results of our analysis applying the $c(M, z)$ proposed by P12 and Macciò et al. (2008), respectively. Subscripts denote the corresponding transformation redshift, z_t . Black dot-dashed lines are the contour of halo mass. Magenta line corresponds to the density peaks, $\delta = \delta_c = 3\sigma(M, z)$, where $\delta_c = 1.69$ and $\sigma(M, z)$ are the critical density peak to collapse and the linear rms fluctuation of the density field for given mass and redshift, respectively. Applying the Press-Schechter theory (Press & Schechter 1974), most of haloes satisfy $\delta < 3\sigma(M, z)$ (below magenta line), stochastically. The yellow and green regions indicate the parameter range satisfying the condition, $t_{\text{cool}} \leq t_{\text{ff}}$, where t_{cool} and t_{ff} are the cooling time and the free-fall time of the gas, respectively. Assuming a total gas mass equal to $0.1 M_{200}$, and a molecular abundance equal to 0.1 per cent of the neutral hydrogen, we estimate the cooling time using the cooling function of primordial gas given by Sutherland & Dopita (1993, yellow) including H_2 cooling (temperature below $\sim 10^4$ K, green) given by Galli & Palla (1998).

A COMMON SURFACE-DENSITY SCALE FOR THE MILKY WAY AND M31 DWARFS

Hayashi & Chiba, ApJ, 803, L11 (2015)

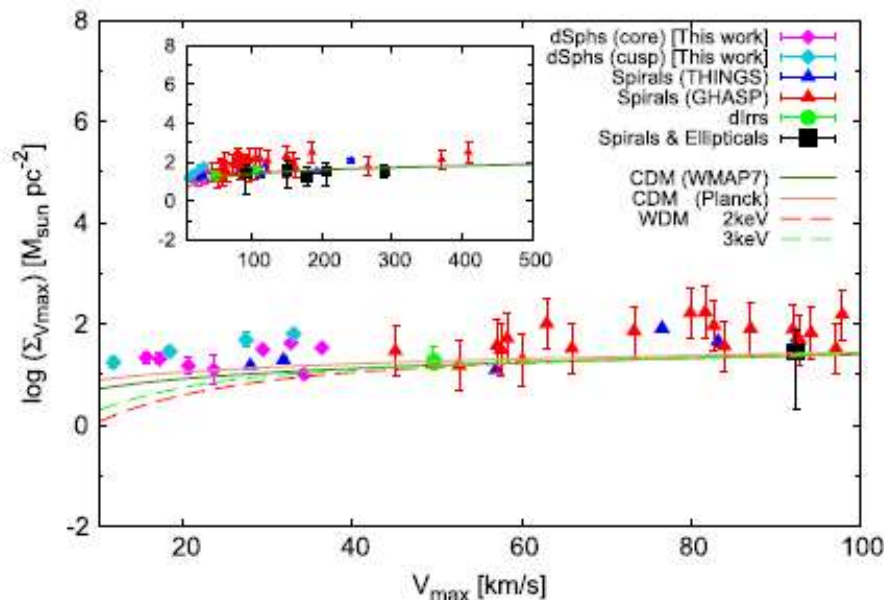


Figure 1. Mean surface density of a dark halo, $\Sigma_{V_{\max}}$, within a radius at maximum circular velocity, V_{\max} , as a function of V_{\max} for different galaxies and Hubble types. While the inset shows all of the samples, as well as CDM (WMAP7) prediction, the main panel highlights the plots only at $V_{\max} \leq 100$ km s⁻¹. Diamonds denote the MW and M31 dSphs derived in K. Hayashi & M. Chiba (2015, in preparation), where magenta and cyan ones correspond to dSphs having a cored and cusped dark halo profile, respectively. Blue and red triangles are the original Spano et al. (2008) sample of spiral galaxy data and nearby spirals in THINGS (de Blok et al. 2008), respectively. The data for dwarf irregular galaxies are indicated by green circles, and spirals and ellipticals investigated by weak lensing are labeled by black squares. Solid lines show the results of CDM models with different cosmological parameters of WMAP7 (dark green) and Planck (orange) measurements. Red and green dashed lines denote WDM models with particle masses of 2 and 3 keV, respectively.

DMHのフィッティング関数に依らない
Scaling Relation

最大のcircular velocity(V_{\max})
の位置(**Rmax**) 内の平均密度 Σ

※DMHのprofileに依らない

$$\Sigma_{V_{\max}} = \frac{M(r_{\max})}{\pi r_{\max}^2},$$

$$M(r_{\max}) = \int_0^{r_{\max}} 4\pi \rho_{\text{dm}}(r') r'^2 dr',$$